Self-organized gold nanoparticles modified HOPG electrodes: Electrochemical stability and its use for electrochemical nanosensing applications

Abdelhafed Taleb, Xue Yanpeng, Pierre Dubot

Self-organized gold nanoparticles modified HOPG electrodes: Electrochemical stability and its use for electrochemical nanosensing applications.

Abdelhafed Taleb[a,b*], Xue Yanpeng[a,b], Pierre Dubot[c]

[a] *PSL Research University, Chimie ParisTech - CNRS, Institut de Recherche de Chimie Paris, 75005, Paris, France*

[b] *Université Pierre et Marie Curie, 4 place Jussieu, 75231 - Paris France.*

[c] *Institut de chimie et des matériaux Paris Est UMR 7181, 2-8 rue Dunant F-94320 Thiais – France.*

ABSTRACT

The presented work shows the development of a performing electrochemical sensor using self-organized gold nanoparticle (Au NP) modified HOPG electrode. Au NPs were functionalized with bisphosphonate-thiol receptors (BP-thiol) whose interactions with Au NP surface were investigated by XPS and FTIR-ATR experiments. It has been shown that the electrochemical stability of modified electrodes increases at potentials higher than -1.3 eV corresponding to the thiol reduction potential. In order to demonstrate the sensing performance of the prepared electrode the electrochemical analysis of copper and silver metal ions was achieved by using square wave voltammetry (SWV). The obtained results show a remarkable performance increase in terms of: the simple fabrication, simple use, and linear behaviour over the concentration range from 5 µM to 0.5 mM, with the detection limit of 5 µM.

KEYWORDS: Au nanoparticles, self-assembly, electrode stability, electrochemical sensor, copper detection

* Corresponding author. Fax: (33)1 44 27 67 50.

E-mail address: abdelhafed.taleb@upmc.fr (A. Taleb)

1. Introduction

The environment and the human health are endangered by the toxicity of some compounds and elements at very low concentration. Heavy metal ions such as Cadmium, Mercury, Cu etc. have been a major concern throughout the world for several decades. Based mainly on possible health risks and contact over a lifetime with an adequate margin of safety, the amount of copper in water for example must be maintained at a concentration of lower than 1.3mg/L ($2.05\ 10^{-5}$ mol L^{-1}) [1]. Drinking contaminated water over a short time causes gastrointestinal distress [2]**.** The regulation requires on one hand a technical treatment to improve the level of technological performance of household plumbing systems against contamination from materials corrosion and on the other hand the development of an efficient sensing system for detection.

However, the development of sensing with high sensitivity has become highly desirable. In this context the use of NPs for new electrode material design is one of the most exciting approaches. Their small size gives them a high surface to volume ratio, which is one of a desired property to construct novel and improved sensing devices [3]. However, nanomaterials have been used to modify metal, glass or carbon in connection with electrochemical [4-17] sensing. Furthermore, the transduction methods based on the electrochemical techniques have optimized conditions for observing and controlling reactions on microsurfaces and nanosurfaces using miniaturized, portable devices [3-16]. Most of the published works, dealing with electrochemical nanosensors, use electrochemistry process for surface nanopatterning. Usually, this process achieves disordered and/or low density surface

structures, because of the preferential nucleation at crystalline defects and step edges of the electrode surface [9-16, 18]. As a consequence of this non accurate control of the electrode surface nanopatterning, it is difficult to control the corresponding specific surface and properties. So far the published works, dealing with the self assembly technique to achieve surface nanopatterning, use surface charged nanoparticles. In this case, the monolayer compactness depends on the nanoparticles size [19] and surface charge. The electrostatic repulsion, between charged nanoparticles, prevents close contact with each other; which in turn reduces the nanoparticles monolayer density. Nanoparticle films for nanotechnological applications such as sensing require, beyond financial aspect, the development of controlled deposition technique (electrode specific surface). However, optimization of sensing material efficiency is a balancing act in which chemical composition and material structure must be taken into account. It is well established that the properties of nanoparticle films in terms of density and structure depend strongly on the used deposition techniques [18]. In utilizing the self assembly technique for nanotechnology devices, one of the important advantages is to distribute nanoparticles uniformly on the substrate with accurate control of density, through the tuning of their concentration, [18] which is a difficult task at the nanometre scale. Furthermore, modification of the electrode surface with self assembled nanoparticles enables to design electrode surface with enhanced specific surface and redox current [20]. In addition, nanomaterials such as Au NPs modifying the HOPG electrode provides the benefit of activating the inhibited sites of terraces basal plane, but have the disadvantage of increasing the energetic barrier for electron transfer between the underlying HOPG electrode and Au NPs due to the Au NPs capping ligands. In previous work, we estimated the electron transfer constant of ferrocyanide oxidation, on bare HOPG and Au NPs modified HOPG electrodes, to be as 1.5×10^{-3} cm s^{-1} and 0.12×10^{-3} cm s^{-1}. [21-22]

Additionally, it is reported that the metal deposition starts at a more positive potential on bare HOPG than on Au NP modified HOPG and that the reduction current is lowered for the Au NP-modified HOPG electrode compared to that for a bare HOPG electrode. These results were attributed to the presence of an n-dodecanethiol layer on Au NPs, which enhance the energetic barrier between the underlying HOPG electrode and Au NPs for the metal ions' reduction [21]. However, this barrier effect of AuNPs is counterbalanced partly by its electro catalytic effect on the inhibited sites of terraces basal plane of HOPG electrode.

The approach adopted in the present work for creating patterned electrode, by using nanoparticles self-assembly, offers many advantages over other methods. First, the nanoparticles are synthesized prior to their deposition, which allows precise control of their size and their packing to maximize the density of their assembly. Furthermore, under the synthesis conditions, the nanoparticles are stable and aggregation is avoided, which increases the preparation reproducibility. This method enables high flexibility for sensing device fabrication.

In this work, we describe for the first time an easy fabrication and use of electrochemical sensors, using controlled closely dense self-organized Au NP modified electrode and BP-thiol molecules as receptors. Additionally, it has been shown that the electrochemical stability of modified electrodes increases at potentials higher than -1.3 eV corresponding to the thiol reduction potential. Furthermore, the properties of the electrochemical sensor were investigated by square wave cyclic voltammetry (SWV). We show very easy fabrication, easy use, controlled properties and sensitive detection of Cu^{2+} and Ag^{+} metal ions. To date, few approaches for the fabrication of nanosenors using nanoelectrodes array with reproducible dimension and repeatable measurements have been reported.

2. Experimental

Metal detection is achieved using a conventional three electrode electrochemical configuration. The reference and counter electrodes were Ag/AgCl and a platinum sheet respectively. As a working electrode we used a clean (0001) highly oriented pyrolytic graphite (HOPG) surface which is produced through a cleaving process. The modified HOPG electrode is prepared by depositing a droplet of Au NP solution on the HOPG surface. The area in contact with the solution is fixed at 9 mm^2 with the help of scotch tape. For metal detection an aqueous solution of 10^{-1} M KNO_3 and different concentrations of metal salts ($CuSO_4$) and/or ($AgNO_3$) were used. By serial dilution, the concentration of copper and/or silver solution was tuned from 10^{-2} to 10^{-7} M. Copper sulphate, silver nitrate, potassium nitrate and n-dodecanethiol are obtained from Fluka whereas (2-((2-mercaptoethyl)thio)ethane-1,1-diyl)diphosphonic acid ($(H_2O_3P)_2CHS(CH)_3SH$, BP-thiol) molecules are obtained from Surfactis technologies. Water used in the preparation of the electrolyte solution was purified by Milli Q System (Millipore, electric resistivity 18.2 MΩ.cm). All measurements were carried out at room temperature.

The 6 nm and 2 nm Au NPs coated with n-dodecanethiol and dispersed in toluene are synthesized by the well known Stucky approach [23], which consists of the chemical reduction of chlorotriphenylphosphine by a ter-butylamine borane complex. The synthesis is achieved in the air by mixing two solutions. The first solution is prepared by adding 0.125ml of dodecanethiol (capping agent) to 0.25mmol of chlorotriphenylphosphine in 20ml of benzene, whereas the second is constituted by 2.5 mmol of ter-butylamine borane complex in 20ml of benzene. The mixed solutions were stirred and heated at a temperature of 55°C during 60min. The color of the solution during this process changes gradually from uncolored to a purple-red solution. For 2 nm Au NPs, the synthesis is achieved by mixing two solutions. A 2mmol of chlorotriphenylphosphine is mixed with 1.2ml of dodecanethiol in 50 ml of chloroform to

prepare the first solution. The second solution is prepared by adding 0.02mol of ter-butylamine borane complex in a mixture of solvents including chloroform (50ml) and ethanol (20ml). The two solutions are mixed and stirred at room temperature for one day to ensure the reaction completion.

Synthesized Au NPs present a narrow size distribution of around 6%. By depositing a droplet of Au NP solution (1.2 10^{-7} M calculated quantitatively from UV-vis spectra using Beer's law [24-25]) on a HOPG electrode, the nanoparticles are organized in a 2D hexagonal structure. The functionalization of self-organized Au NPs modified HOPG electrode is achieved by immersing the electrode into an aqueous solution of BP-thiol with a concentration of 10^{-2} M for 20 hours.

The electrochemical measurements (square wave voltammetry (SWV)) are performed with a Voltalab PGZ301 potentiostat and carried out at room temperature. The used parameters of the SWV experiments were as follows: E_{begin}= -0.6V, E_{end}= 0.6, ΔE=50mV, E_s=2mV, t_{eq}=5s.

Morphology of the self-assembled Au NPs on the HOPG electrode is characterized using a transmission electron microscope (JEOL 100CX) operated at 100 kV. The transmission electron microscope (TEM) grids are prepared by sticking a thick leaf of cleaved graphite on bare copper grids (without carbon film). By repeating the cleaving process a thinner slices of transparent HOPG for TEM measurements are obtained. The HOPG cleaving is performed with the help of scotch tape. A piece of tape is pressed onto the surface of HOPG and after pulling it off, the tape takes with it a thin layer of HOPG. The morphological investigations of the self-assembled Au NPs monolayer on the HOPG electrode were achieved also with a high-resolution Ultra 55 Zeiss FEG scanning electron microscope (FEGSEM) operating at an acceleration voltage of 10 kV.

The chemical composition of the samples is determined by X-ray photoelectron spectroscopy (XPS) and the measurements are performed on a thermo VG Scientific ESCALAB 250 system fitted with a microfocused, monochromatic Al Kα X-ray source (hυ = 1486.6 eV; spot size 650 μm, power=15 kV x 200 W).

Fourier transform infrared in attenuated total reflectance mode (FTIR-ATR) experiments were conducted with a dry-air-purged Thermo Scientific Nicolet 6700 FTIR equipped with a Mercury Cadmium Telluride (MCT) detector. Spectral resolution was 4 cm^{-1}, and spectra were averaged from 256 scans. The ATR accessory is a horizontal ZnSe crystal coated with diamond (A = 2.54 mm^2) with single reflection and an angle of incidence of 45° (Smart MIRacle ATR accessory from PIKE Technologies company). For data reprocessing, OMNIC software was used.

3. Results and discussion

The fabrication of a sensor electrode is achieved through two steps: modification of the HOPG electrode with self-organized Au NPs and functionalization of the Au NPs surface with BP-thiol molecules. The modified HOPG electrode is prepared through the deposition of a droplet of Au NP solution on the HOPG surface, which then self-organizes as a hexagonal structure (Fig. 1). It has been shown that the NP' size, shape and surfactant shell are the main parameters determining the structure formed in the self-assembly process [26-33]. Thus for ordered close-packed nanoparticle arrays with long range, from a few to several tens of microns, both with a narrow size distribution, uniform morphology and adequate capping ligand surface coverage are required [26-33]. However, the packing arrangements and the densities of the NPs depend on their radius and the ligand length [27, 29, 31]. Different lengths of alkylthiol ligand have been used to stabilize Au NPs [31]. An adequate choice of

nanoparticle capping ligands is necessary, because it plays different roles: [31-33] (i) it prevents coalescence between nanoparticles, (ii) it fixes the distance between nanoparticles and (iii) it acts as a lubricating agent between nanoparticles and electrode surface; which favours nanoparticles diffusion to form a well-organized arrangement over a long distance.

In our case the optimum conditions for the formation of a close 2D hexagonal array, with high degree and long range ordering respecting the arguments mentioned above, are obtained using n-dodecanethiols ($C_{12}SH$). The long range ordering depends also on the concentration of NP solution before deposition, and is crucial for surface nanostructuring and development of sensing applications.

The structural parameters of the organized arrays of $C_{12}SH$ -capped Au NPs depend on the configuration of the $C_{12}SH$ alkyl chain. The calculated value of the $C_{12}SH$ length tail from the Bain equation [32] is found to be equal to 1.77 nm, which is in good agreement with the inter-NPs distance obtained from TEM experiments ranging from 1.8 to 2 nm (Fig1). This result suggests the intercalation or interpenetration of individual or domains of chains along the directions of neighboring Au NPs to form more compact bundles than the alkyl groups on the top of the nanoparticles (insert Fig. 1). Assuming the inter-NP distance is equal to 1.8 nm and hexagonal packing structure, the HOPG surface coverage of 2.8×10^{12} NPs cm^{-2} is expected.

Another role of the nanoparticles capping ligands, not mentioned above and discussed below, is the nanoparticles adhesion to the electrode surface, when it is immersed into aqueous solution. In order to minimize hydrophobic interaction of dodecanethiol molecules with the electrolyte, it does probably diffuse to a region between nanoparticles leaving the top surface of the nanoparticules, free of thiols and in contact with the solution [18]. These dodecanethiol molecules form a dense interpenetrating chain region between nanoparticles (insert Fig. 1); which in one hand do ensure mechanical stability of the self-assembled

structure [34], and in the other hand do act as an isolating hydrophobic region which ensures nanoparticles adhesion to the electrode surface. Furthermore, even though these ligands favour nanopartiticle adhesion, they reduce drastically their surface in contact with the solution. Modified electrodes with dodecanethiol coated nanoparticles were tested in different conditions of temperature and immersion time and they have shown stable behaviour [35].

The stability of modified electrodes with dodecanethiol functionalized nanoparticles coating was demonstrated to depend on the thiol adsorption strength on Au nanoparticles. It is well known that sulphur group manifests strong affinity to metal surface with predominantly covalent bounding and scarcely polar bounding [36-37]. In fact, the thiol adsorption rate is strongly influenced by various parameters such as the applied potential [37], the temperature [39], the substrate surface and the electrolyte nature and concentration. However, it is well established that the thiol adsorption is favoured by slightly positive potential around the open circuit one, whereas negative potential accelerates thiol desorption [38].

To select the applied potential for our experiments, cyclic voltammetry measurements in different conditions of applied potential and immersion time were tested. It could be observed from Figure 2 that the reductive desorption of dodecanethiol starts at potential of -1.1V with a reductive desorption peak at -1.3V for the first sweep [40]. A small reductive desorption peak is observed for other sweeps, which is attributed to desorption of dodecanethiol adsorbed when the potential is above -1.1V.

To check more the stability of modified electrodes, FEGSEM characterizations were achieved. The obtained results are presented in Figure 3. The FEGSEM images correspond to modified electrodes with dodecanethiol functionalized nanoparticles coating and polarized under different potentials -0.7V, -1V and -1.4V for 1200s. Clearly, it could be observed that

when the applied potential is shifted to more negative ones (Fig 3(a) and (b)), the nanoparticle rate coverage decreases. In fact, hole defects appear in the nanoparticles monolayer, which size and density increase with the potential shifts to the negative region (Fig 3(a) and (b)). For high negative potential around -1.4V (Fig.3(c)), it has been observed that the rate coverage of the electrode is considerably reduced and Au NPs coalescence takes place. These outcomes are a consequence of reductive desorption of dodecanethiol from Au NPs surface, which induces their detachment from the electrode surface and their diffusion into the bulk solution for some of them, and for others when they get into contact they coalesce. As it should be observed from Figure 2, the reduction desorption of dodecanethiol depends also on the Au NP size. For small Au NPs of 2nm, desorption potential is shifted to more positive potentials. This should prone different desorption kinetics, which in turn favours different dodecanethiol rate coverages at a given potential depending on the nanoparticles size. At given applied potential within the negative range, a small nanoparticle will coalesce first leaving the larger nanoparticles to coalesce in later stage, which explain different nanomaterial size observed in Figure 3(c).

In a previous published work by using cyclic voltammetry at temperature lower than 82°C which is the thiol desorption temperature [35], it is demonstrated that after 50 repetitive sweeps at a scan rate of 100mV/s the peak current intensity and position of silver oxidation and reduction keep the same value. This indicates that the Au NPs modified electrode has good electrochemical properties and that the Au NPs act as the electron mediators and favor electron transfer between the metal ion and the electrode. These results are completed and confirmed by the present experiments.

Au NPs functionalization with BP-thiol molecules was achieved by soaking the Au NPs modified HOPG electrode in a 10^{-2} M BP-thiol solution for 20 hours. BP-thiol molecules could get attached to the Au NPs' surface through the thiol group [26-33] or phosphonate

groups [41-45] in a competitive manner. To confirm one of the scenarios, the XPS analyses have been performed. It should be noted that on the XPS spectrum obtained after functionalization (Fig. 4a) a phosphorus signal appears (curve in green, Fig. 4a), whereas it is absent in the spectrum before functionalization (curve in black, Fig. 4a), corresponding to the signature of BP-thiol ligands' fixation on Au NPs surface. It is interesting to see that after immersing modified electrode in a metal solution (curve in blue, Fig. 4b) and performing the SWV experiments (curve in red, Fig. 4b) a new peak appears at around 168.2 eV as a consequence of Cu^{2+} ions interaction with the electrode. This new peak is well known to correspond to oxidized thiol ($R\text{-}SO_3^-$, $R\text{-}SO_4^-$) and has been observed with thiol bonding to silver or copper [18, 46-48]. Furthermore in the case of copper, this oxidation is well known to be accompanied by the reduction of Cu^{2+} either to the Cu^+ or Cu^0 (metallic copper) oxidation state, which manifests the same XPS spectra [49]. Additionally, just after Au NPs functionalization with BP-thiol molecules, this peak at around 168.2 eV is absent (curve in red, Fig4b), whereas the peak at around 163,8eV corresponding to unbounded thiol is intense. It should be noted that the signal corresponding to the S2p orbital is typical of the one observed for metal covered by SAM, and can be fitted by two doublet components located at around 162.6 eV and 165 eV [50-51]. The first component located at 162.6 eV is assigned to adsorbed dodecanethiol molecules on Au NPs surface, while the second component located at 165 eV is attributed to free thiol molecules. This is in accordance with the fact that the HOPG electrode is modified by Au NPs covered with dodecanethiol and BP-thiol molecules. The radiation damage during XPS experiments on dodecanethiols capped Au NPs, results in dodecanethiol desorption but not the formation of adherent oxidized thiols on Au NPs [52-53]. However, the analysis of the two peaks of S2p was unable to distinguish between thiol groups belonging to BP-thiol and dodecanethiol molecules.

After the immersion of the modified electrode into Cu and/or Ag ions solution, the characteristic peaks of Cu2p, Ag3d (Fig 5(a) and (b)) and oxidized forms of thiols (Fig. 4(b), blue curve) do appear. This peak remain after SWV measurement and show a good similarity with the one observed from the Cu NPs coated with n- dodecanethiol [46-48], which undoubtedly prone the complexation of thiol head group with Cu^{2+} ions. One plausible explanation to these XPS results is that the S is bound to Cu and this thiol get oxidized in later stage as manifested by the appearance of oxidized thiol peak.

Furthermore, the XPS signal corresponding to P_{2p} core level remains constant after immersing the electrode in Cu solution (curve in blue) and after SWV experiments (curve in red) (Fig. 4a), which means that the phosphonate group keeps the same chemical environment. However, one explanation for these results is that the thiol group is bound to Cu and evolves toward oxidized thiol in the later stage as previously observed by different authors [18, 46-48]. These results demonstrate thiol interaction with Cu^{2+} ions in solution, and suggest the fact that the phosphate groups bond to the Au NP surface.

Further evidence of phosphonate group interaction with Au NPs surface, is provided by FTIR-ATR experiments. By comparison with the solution spectra, it appears that both peaks located at 1060 cm^{-1} and 1170 cm^{-1} are slightly shifted by around 25 $cm^{-1}$and that there is an increase of the half band width (fwhm) when BP-thiol is interacted with Au NPs surface (Fig. 6), meaning that the chemical environment of BP-thiol molecules changed after the interaction with Au NPs. Generally, when species are adsorbed onto solid surface as an inner-sphere complex, the symmetry is reduced in comparison with the free species, leading to characteristic changes in the IR spectra [54]. Therefore, the observed IR signal can be interpreted as strong interaction of BP-thiol molecules with Au NP surface.

For the free BP-thiol molecules (red line), decomposition of band between 900 to 1300cm^{-1}, corresponds to the P-O stretching vibration. The peaks located at 1170 and 920cm-1 correspond to P=O and P-OH respectively [55], whereas the one located at 1060 is assigned to the vibrational mode for the PO_3 group [56]. Furthermore, the peaks between 1400 and 1500 cm^{-1} correspond to C-H vibration modes. The location of these peaks is similar to those obtained with free bisphosphonate functional group on Au NP [57].

After socking the Au NP modified HOPG electrode into BP-thiol solution and washing it with deionized water to remove none adsorbed molecules, the FTIR spectra show large changes within P-O stretching region (900-1250cm^{-1}). These results are a signature of the interaction between the phosphonate group of BP-thiol molecules and Au NP surface, which result in binding formation between the phosphonate groups and Au atoms within Au NP surface. In fact, the phosphonate group can bond to Au NP surface as a hydrogen bond donor through the P-OH group and/or as acceptor via P=O oxygen [58]. Different changes observed after phosphonate group bonding to Au NP surface are consistent with the results of previous published works by Fiurasek et al. [57].

For metal accumulation, the functionalized self-organized Au NPs modified HOPG electrode was immersed in a solution containing metal salt with different concentrations at an open circuit potential for 10 min. After removal of the electrode from the metal ion solution, it is rinsed with ionised water and then immersed in a metal free solution for electrochemical measurements using SWV technique, which is more sensitive than cyclic voltammetry [59]. For Au NPs without BP-thiol ligands, no current peak is observed under the same conditions (Fig.7). Furthermore, for BP-thiol functionalized electrode it can be observed that in the potential region of -0.4 to +0.6 V there is a SWV peak, which intensity depends on the Cu^{2+} (Fig. 8a) concentration. This indicates that there is no interaction between Cu^{2+} ions and the Au NP surface and that the appearance of the SWV peak is ascribed to the interaction

between BP-thiol ligands and Cu^{2+} ions. In the absence of accumulated metal no current response is observed (Fig. 8a), which confirms that the redox peaks are due to the oxidation and reduction of accumulated metal from the metal solution.

To examine the selectivity of functionalized Au NPs modified HOPG electrode, the voltammograms of Co^{2+} and Ni^{2+} metal ions were analyzed. The results show no discernible peak, which indicates a weak interaction between the functionalized Au NPs modified HOPG electrode and these metal ions. This behavior could be explained by the higher interaction of thiol with copper [48]. To confirm this hypothesis, prepared sensors were used to detect silvers ions. The results are depicted in Figure 8(b) which show an efficient detection toward silver ions. The attempt to detect other metals than Ag^{+} and Cu^{2+}, which have a weak interaction with thiol has been not successful. This is chiefly due to the weak interaction between sulfur and other metals [60]. These results demonstrate that the prepared system is efficient to detect metal ions, which have strong interaction with thiol such as Ag^{+} and Cu^{2+} ions at low concentrations. In addition, the selectivity toward each metal ion is achieved by the fact that each metal ion has a defined redox potential. Furthermore, from Fig. 8 it could be observed that this sensor system enables multiple metal ions detection. It had high sensitivity toward Ag^{+} ions which is five time that of Cu^{2+} ions.

Insert of Figs. 8a, 8b and 9 shows the calibration curve corresponding to functionalized Au NPs modified HOPG electrode. It should be noted a linear relationship between the current response and metal ions concentration within the range of 5×10^{-6} M and 5×10^{-2} M, with the detection limit of 5 μM.

Furthermore, the capture and delivery of the copper ion could be achieved only by tuning the potential. The regeneration of the prepared electrode is performed easily by applying positive potential of 0.4 V over 600s to oxidize deposited copper. The main limitation of the electrode

repeatability is the receptor molecules desorption on the surface of Au nanoparticles modified HOPG. This depends on the temperature and the applied potential as mentioned in the first part of the discussion section.

4. Conclusion

The reported results demonstrate for the first time the potential of BP-thiol ligands functionalized self organized Au NPs modified HOPG electrode to be used as a sensor for Ag^{+} and Cu^{2+} ions detection. However, the considered system could be extended to detect other metal ions which have strong interactions with thiol group. The prepared electrode for sensing applications showed high performance in terms of ease of fabrication and use, low cost and linear behaviour over the concentration range from 5 µM and 0.5 mM, with the detection limit of 5 µM. The selectivity was demonstrated to be toward metal ions with strong interaction with thiol group such as Ag^{+} and Cu^{2+} ions. However, closely dense self-assembled Au NPs platforms have a promising future in the design of electrochemical sensor applications with controlled properties. Different published works using Au NPs showed that it is possible to detect various chemical species [3, 7-8, 10, 61-63], by using a convenient receptors. Based on these works, it is expected that this principle can be directed toward other transcription factors by simply changing the recognition sequence. The present electrochemical sensors provide the advantage of enabling multi ions detection but suffer from weak selectivity toward a given ion. In fact, the selective detection efficiency is based on a specific interaction between the receptor and targeted species to detect in a given environment. For example, to improve the selectivity of prepared sensor platform toward copper ion detection, a cyclam molecules could be a convenient receptor. Different recent works reported the efficiency of this receptor to detect specifically copper ions [64-66].

Acknowledgement

We are grateful to Gregory Lefevre at the PSL Research University, Chimie ParisTech - CNRS, Institut de Recherche de Chimie Paris for performing and discussing the FTIR-ATR spectra. We would like also to thank Dr. David Portet at Surfactis Technologie, 22 rue Roger Amsler, 49100 Angers, France for providing BP-molecules.

Figure captions

Fig. 1: TEM image of self-organized Au NPs in a 2D hexagonal structure, (a) Au NPs of 6nm and the inserts is the schematic illustration of the hexagonal structure of the Au NPs monolayer showing dense bundles of $C_{12}SH$ ligands between NPs (b) a magnification of Au NPs of 6 nm and (c) self-organized 2 nm Au NPs in a 2D hexagonal structure.

Fig. 2: Voltammogram of modified HOPG electrode with self assembles Au NPs monolayer in the electrolyte aqueous solution of 10^{-1} M KNO_3 at different indicated potentials and immersion time of 1200s.

Fig. 3: FEGSEM images of modified HOPG electrode with self assembles Au NPs monolayer at different indicated potentials and immersion time of 1200s.

Fig. 4: High resolution XPS spectra of P2p core level in the following situations (a): Au NP-modified HOPG without BP-thiol functionalization (black curve), after BP-thiol

functionalization (green curve), after electrode immersion into Cu ions solution (red curve) and after SWV measurements (blue curve). (b) Spectra of S2p core level in the following situations: Au NP-modified HOPG after BP-thiol functionalization (red curve), after electrode immersion into Cu ions solution (blue curve) and after SWV measurements (green curve).

Fig. 5: High resolution XPS spectra of Ag3d (a) and Cu2p (b) after BP-thiol functionalized electrode immersion in Cu^{2+} (a) or Ag^{+} (b) solution and SWV experiments.

Fig.6: ATR-FTIR spectra of BP-thiol (free ligand, red line) and after the interaction with Au NPs (blue line).

Fig.7: SWV voltammograms of Au NP-modified HOPG electrode without BP-thiol functionalization, recorded with a scan rate of 10 mV s^{-1}, in aqueous solution of KNO_3 (10^{-1}M) free of Cu^{2+} and Ag^{+} and after immersion in Ag^{+} and Cu^{2+} solution of indicated concentration.

Fig.8: SWV peaks of an Au NP-modified HOPG electrode with BP-thiol functionalization, recorded with a scan rate of 10 mV s^{-1}. (a) In aqueous solution of KNO_3 (10^{-1}M) free of Cu^{2+} and after immersion in Cu^{2+} solution of indicated concentration. The inserts show high magnification of indicated zone and plot of SWV peaks current versus Cu^{2+} solution concentration. (b) The same experiments with Ag^{+} solution. The inserts are plots of SWV peaks current versus Ag^{+} solution concentration and magnification of indicated zone.

Fig.9: SWV voltammograms of an Au NP-modified HOPG electrode with BP-thiol functionalization, recorded with a scan rate of 10 mV s^{-1}. (a) In aqueous solution of KNO_3 (10^{-1}M) free of Cu^{2+} and Ag^{+} and after immersion in Ag^{+} and Cu^{2+} solution of indicated concentration.

References

[1] D. Larry Sparks, B. G. Schreurs, *Proceeding of the national academy of Science of the united states of America,* 2003**, 100**, 11065-11069.

[2] C. D. Klaassen, *Casarett and Doull's Toxicology: The Basic Science of Poisons,* Eds. McGraw-Hill Publishing Co., Inc., 7rd, ed.; New York, 2008.

[3] X. Luo, A. Morrin, A. J. Killers, M. R. Smith, Application of nanoparticles in electrochemical sensors and biosensors, *Electroanalysis*, 2006, **18**, 319-326.

[4] J. Luo, S. Jiang, H. Zhang, J. Jiang, X. A. Liu, novel non enzymatic glucose sensor based on Cu nanoparticles modified graphene sheets electrode, *Analytica Acta*, 2012, **709**, 47-53.

[5] J. Wang, C. Bian, J. Tong, J. Sun, S.; Xia, L-Aspartic acid/L-cysteine/gold nanoparticle modified microelectrode for simulation detection of copper and lead, *Thin Solid Film*, 2012, **520**, 6658-6663.

[6] M. H. Mashhadizadeh, S. Ramezani, S. Ebrahimi, Potentiometric determination of nanomolar concentration of Cu (II) using a carbon paste electrode modified by a self assembled mercapto compound on gold nanoparticles, *Sensors and Actuators B,* 2012, **169**, 305-311.

[7] Y. Cui, C. Yang, W. Zeng, M. Oyama, W. Pu, Y. Zheng, J. Zhang, Three dimensional Monolayer of 3 Mercaptopropionic acid assembled on gold nanoparticles for electrochemical determination of trace Cu(I), *Analytica Letters*, 2007, **40**, 2140-2160.

[8] C. Berghian Grosan, C. Varodi, A. Vulcu, L. Olenic, S. Pruneanu, V. Almasan, Structural and electrochemical characterization of novel leucine gold nanoparticles modified electrode, *Electrochemica Acta*, 2012, **63**, 146-152.

[9] S. Wang, Y. Wang, L. Zhou, J. Li, S. Wang, H. Liu, Fabrication of an effective electrochemical platform based on graphene and AuNPs for high sensitive detection of trace Cu^{2+}, *Electrochemica Acta*, 2014, **132**, 305-311.

[10] K. Kerman, M. Saito, S. Yamamura, Y. Takamura, E. Tamiya, Nanomaterial-based electrochemical biosensors for medical applications, *Trends in Analytical Chemistry*, 2007, **27**, 585-592.

[11] A. Merkoçi, Elecrochemical biosensing with nanoparticles, *FEBS Journal*, 2007, **274**, 310-316.

[12] J. M. Pingarron, P. Yanez-Sedeno, A. Gorzalez-Cortes, Gold nanoparticle-based electrochemical biosensors, *Electrochemica Acta*, 2008, **53**, 5848-5866.

[13] Y. Y. Xu, C. Brian, S. Chen, S. Xia, A microelectronic technology based amperometric immunosensor for α-fetoprotein using mixed self-assembled monolayers and gold nanoparticles, *Anal. Chem. Acta*, 2006, **561**, 48-54.

[14] A. Yu, Z. Liang, J. Cho, F. Caruso, Nanostructured electrochemical sensor based on dense gold nanoparticle films, *Nano Lett.*, 2003, **3**, 1203-1207.

[15] J. Lia, B. Wang, A. Wu, G. Cheng, Z. Li, A. Dong, A method to construct a third generation horseradish peroxidase biosensor: self-assembling gold nanoparticles to three dimensional sol-gel network, *Anal. Chem.*, 2002, **74**, 2217- 2223.

[16] C. Carralero, M. L. Mena, A. Gonzalez-Cortés, P. Yanez-Sedeno, L. M. Pingarron, Development of a tyrosinase biosensor based on gold nanoparticles-modified glassy carbon electrodes. Application to the measurement of a bioelectrochemical polyphenols index in wines, *Anal. Chim. Acta*, 2005, **528**, 1-8.

[17] E. H. El-Ads, A. Galal, N. F. Atta, Electrochemistry of glucose at gold nanoparticles modified graphite/SrPdO3 electrode-Towards a novel non enzymatic glucose sensor. *J. Electroanal. Chem.* 2015, **749**, 42-52.

[18] A. Taleb, C. Mangeney, V. Ivanova. Metallic nanostructure formation using self-assembled Chemically Anchored Gold Nanoparticles, *J. Electrochem. Soc*., 2011, **158**, K28-K34.

[19] A. Doron, E. Katz, I. Willner, Organization of Au colloids as monolayer films onto ITO glass surface: Application of metal colloid films as Base interface to construct redox active monolayers, *Langmuir*, 1996, **11**, 1313-1317.

[20] K. R. Ward, M. Gara, N. S. Lawrence, R. S. Hartshorne, R. G. Compton, R. G. Nanoparticle modified electrodes can show an apparent increase in electrode kinetics due solely to altered surface geometry: The effective electrochemical rate constant for non -flat and non-uniform electrode surfaces, *J. Electroanal. Chem.*, 2013, **695**, 1-9.

[21] A. Taleb, X. Yanpeng, P. Dubot, Self-organized gold nanoparticles as new nanoelectrocatalyst templates for surface nanostructuring, *J. Electroanal. Chem.*, 2013, 693, 60-66.

[22] A. Taleb, A. O. Gusev, F. Silly, F. Charra and M. P. Pileni, Electron transport properties of nanocrystals: Isolated or in "supra" crystalline phases, *Adv. Mat.*, 2000, 12, 633-637.

[23] Zheng, N.; Fan, J.; Stucky, G. One-step one-phase synthesis of monodisperse noble-metallic nanoparticles and their colloidal crystals. *J. Am. Chem. Soc*. **2006**, 128, 6550-6551.

[24] W. Haiss, N. T. K. Thanh, J. Aveyard, D. G. Fernig, Determination of Size and Concentration of Gold Nanoparticles from UV-Vis Spectra, *Annal. Chem.*, 2007, **79**, 4215-4221.

[25] S. Link, M. A. El-Sayed, Spectral properties and relaxation dynamic of surface plasmon electronic oscillations in gold and silver nanodots and nanorods, *J. Phys. Chem.*, 1999, **103**, 8410-8426.

[26] Z. L. Wang, Structural Analysis of Self-Assembling Nanocrystal Superlattices, *Adv. Mater.*, 1998, **10**, 13-30.

[27] L. Motte. F. Billoudet, M. P. Pileni, Self-assembled monolayer of nanosized particles differing by their sizes, *J. Phys. Chem.*, 1995, **99**, 16425-16429.

[28] S. A. Harfenist, Z. L. Wang, R. I. Whetten, I. Vezmar, M. M. Alvarez, Three dimentional hexagonal close packed superlattice of passivated Ag nanocrystals, *Adv. Mater*., 1997, **9**, 817-822.

[29] K. Vijaya Sarathy, G. Raina, R. T. Yadav, G. U. Kulkarni, C. N. R. Rao, Thiol-Derivatized Nanocrystalline Arrays of Gold, Silvers, and platinum, *J. Phys. Chem. B,* 1997, **101**, 9876-9880.

[30] A. Taleb. C. Petit, M. P. Pileni, Synthesis of highly monodisperse silver nanoparticles from AOT reverse micelles: a way to 2D and 3D self-organization, *Chem. Mater.*, 1997, **9**, 950-959.

[31] L. Motte, M. P. Pileni, Self-assemblies of silver sulfide nanocrystals: influence of length of thio-alkyl chains used as coating agent, *Appl. Surf. Sci.*, 2000, **164**, 60-67.

[32] C. D. Bain, E. B. Troughton, Y. T. Tao, J. Evall, M. G. Whitesides, R. G. Nuzzu, Formation of monolayer films by the spontaneous assembly of organic thiols from solution onto gold, *J. Am. Chem. Soc.*, 1989, **111**, 321-335.

[33] B. A. Borgel, S. Fullam, S. Connolly, D. Fitzmaurice, Assembly and self-organisation of silver nanocrystal superlattices: Ordered soft spheres, *J. Phys. Chem. B,* 1998, **102**, 8379-8388.

[34] A. O. Gusev, A. Taleb, F. Silly. F. Charra, M. P. Pileni, Inhomogeneous Photon Emission Properties of Self-Assembled Metallic Nanocrystals, *Adv. Mat.*, 2000, **12**, 1581-1583.

[35] A. Taleb, X.; Yanpeng, S. Munteanu, F. Kanoufi, P. Dubot, Self-assembled thiolate functionalized gold nanoparticles template toward tailoring the morphology of electrochemically deposited silver nanostructure, *Electrochimica Acta,* 2013, **88**, 621– 631.

[36] C. E. D. Chidsey, C. R. Bertozzi, T. M. Putvinski, A. M. Mulsce, Coadsorption of ferrocene-terminated and unsubstituted alkanethiols on gold: electroactive self-assembled monolayers, *J. Am. Chem. Soc.*, 1990, **112**, 4301- 4306.

[37] S. Arnold, Z. Q. Feng, T. Kakiuchi, W. Knoll, K. Niki, Investigation of the electrode reaction of cytochrome *c* through mixed self-assembled monolayers of alkanethiols on gold (111) surfaces, *J. Electroanal. Chem.*, 1997, **438**, 91.

[38] R. Meunier-Prest, G. Legay, S. Raveau, N. Chiffot, E. Finot, Potential-assisted deposition of mixed alkanethiol self-assembled monolayers,

Electrochemica Acta, 2010, **55**, 2712-2720

[39] I. Robel, X. Lin, M. Sprung, J. Wang, Thermal stability of two-dimentional gold nanocrystal superlattices, *J. Phys.: Condens. Matter,* 2009, **21**, 264011.

[40] C. M. A. Brett, S. Kresak, T. Hianik, A. M. O. Brett, Studies on self-assembled alkanethiol monolayers formed at applied potential on polycrystalline gold electrodes, *Electroanalysis*, 2003, **15**, 5-6.

[41] I. Felhosi, R. Ekes, P. Baradlai, G. Palinkas, K. Varga, E. Kalman, Coupled radiotracer and voltammetric study of the adsorption of 1-hydroxy-ethane-1,1-diphosphonic acid on polycrystalline gold, *J. Electroanal. Chem.,* 2000, **480**, 199-208.

[42] W. Fritzsche, T. A. Taton, Metal nanoparticles as labels for heterogeneous, chip-based DNA detection, *Nanotechnology,* 2003, **14,** R63-R73.

[43] E. Gumienna-Kontecka, J. Jezierska, M. Lecouvey, Y. Leroux, H. Kozlowski, Bisphosphonate chelating agents: Coordination ability of 1-phenyl-1-hydroxymethylene bisphosphonate towards Cu^{2+} ions, *J. Inorganic Biochemistry*, 2002, **89**, 13-17.

[44] W. Yang, W.; Jaramillo, D.; Justin Gooding, J.; Brynn Hibbert, D.; Zhang, R.; Willet, G. D.; Fisher, K. J. Sub-ppt detection limits for copper ions with Gly-Gly-His modified electrodes. *Chem. Commun*. **2001**, 19, 1982-1983.

[45] M. Dyba, M. Jezowska-Bojczuk, E. Kiss, T. Kiss, H. Kozlowski, Y. Leroux, D. E. Manouni, 1-Hydroxyalkane-1,l-diyldiphosphonates as potent chelating agents for metal ions. Potentiometric and spectroscopic studies of copper (II) coordination, *J. Chem. Soc. Dalton Trans,* 1996, **6**, 1119-1123.

[46] N. S. Pesika, F. Fan. P. C. Searson, K. J. Stebe, Site-Selective Patterning Using Surfactant-Based Resists, *J. Am. Chem. Soc*, 2005, **127**, 11960-11962.

[47] A. Taleb, X. Yanpeng, Electrodeposition of self-organized superstructure of copper dendrites or polyhedral particles on gold nanoparticle modified highly oriented pyrolytic graphite electrode, *Electrochimica Acta*, 2013, **112**, 838– 844.

[48] P. E. laibinis, G. M. Whitesides, D. L. Allara, Y. T. Tao, A. N. Parikh, R. G. Nuzzo, Comparison of the structure and wetting properties of self assembled monolayers of n-alkanethiols on the coinage metal surfaces, copper, silver and gold, *J. Am. Chem. Soc.*, 1991, **113**, 7152-7167.

[49] Y. Wang, J. Im, J. W. Soares, D. M. Steeves, J. Whitten, Thiol adsorption on and reduction of copper oxide particles and surfaces, Langmuir, 2016, **32**, 3848-3857

[50] M. A. D. Millone, H. Hamoudi, L. Rodriguez, A. Rubert, G. A. Benitez, M. E. Vela, R. C. Salvarezza, J. E. Gayone, R. C. Sanchez, O. Grizzi, C. Dablemont, V. A. Esaulov, Self-Assembly of Alkanedithiols on Au(111) from Solution: Effect of Chain Length and Self-Assembly Conditions, *Langmuir*, 2009, **25**, 12945- 12953.

[51] B. J. Lindberg, K. Hamrin, G. Johansson, U. Gelius, A. Fahlman, C. Nordling, K. Siegbahn, Molecular spectroscopy by means of ESCA II. Sulfur compounds. Correlation of electron binding energy with structure, *Phys. Scr.*, 1970, **1**, 286-298.

[52] T. M. Willey, A. L. Vance, T. Van Buuren, C. Bostedt, L. J. Terminello, C. S. Fadley, Rapid degradation of alkanethiol-based self-assembled monolayers on gold in ambient laboratory conditions, *Surface science*, 2005, **576**, 188-196.

[53] J. M. Ramallo-Lopez, L. J. Giovanetti, F. C. Vicentin, F. G. Requejo, XANES study of the radiation damage on alkanethiolates capped Au Nanoparticles, *J. Physics: Conference series*, 2013, **430**, 012034.

[54] K. Müller, G. Lefevre, Vibrational characteristics of outer sphere surface complexes: example of sulfate ions adsorbed onto metal hydroxides, *Langmuir*, 2011, **27**, 6830-6835.

[55] R. D. Peacock, The intensities of lanthanides f-f transitions, *Structure and Bonding*, 1975, **22**, 83-122.

[56] E. Podstawka, R. Borszowska, M. Grabowska, M. Drag, P. Kafarski, L. M. Proniewicz, Interaction of molecular structures and adsorption mechanisms of phosphonodipeptides by surface-enhanced Raman, Raman and infrared spectroscopies, *Surface Science*, 2006, **599**, 207-220.

[57] P. Fiurasek, L. Reven, phosphonic and sulfonic acid functionalized gold nanoparticles a solid state NMR study, Langmuir, 2007, **23**, 2857-2866.

[58] A. Mahmoudkhani, V. Langer, phenylphosphonic acid as a building block for two dimensional hydrogen-bonded supramolecular arrays, Mol. Struct. 2002, **609**, 97-108.

[59] G. R. Xu, Y. Yuan, S. Kim, J. J. Lee, Surface modification of gold by quercetin monolayer for the electrochemical determination of copper (II), *Electroanalysis*, 2008, **10**, 1690-1695.

[60] Y. L. Hung, T. M. Hsiung, Y. Y. Chen, Y. F. Huang, C. C. Huang, Colorimetric detection of heavy metal ions using label free gold nanoparticles and alkanethiols, *J. Phys. Chem. C,* 2010, **114**, 1629-16334.

[61] I. Turyan, D. Mandler, Low-Level Mercury Electrochemical Detection, *Nature*, 1993, **362**, 703-704.

[62] N. Ratner, D. Mandler, Electrochemical detection of low concentration of Mercury in water using gold nanoparticles, *Anal Chem.*, 2015, **87**, 5148-5155

[63] I. Willner, B. Willner, Biomolecule-based nanomaterials and nanostructures, *Nano Lett.*, 2010, **10**, 3805-3815.

[64] S. Goubert-Renaudin, M. Etienne, S. Brabdes, M. Meyer, F. Denat, B. Lebeau, A. Walcarius. Factors affecting copper (II) binding to multiarmed cyclam-grafted mesoporous silica in aqueous solution, *Langmuir*, 2009, 25, 9804-9813.

[65] S. Goubert-Renaudin, M. Etienne, Y. Rousselin, F. Denat, B. Lebeau, A. Walcarius, Cyclam-functionalized silica-modified electrodes for selective determination of Cu(II), *Electroanalysis*, 2009, 21, 280-289.

[66] B. Feier, L. Fizesan, C. Mériadec, S. Ababou, Girard, C. Cristea, R. Sandulescu, F. Genest, Influence of the electrografting methods on the performances of a flow electrochemical sensor using modified electrodes for trace analysis of copper (II). *Journal of electroanalytical chemistry*, 2015, 744, 1-7.

High lights

- Self-organized gold nanoparticles modified HOPG was demonstrated to be electrochemically stable electrode for potential higher than the desorption potential of dodecanethiol.

- Prepared electrodes were shown to be potential electrode material for electrochemical nanosensing applications.

- The obtained results show remarkable performance increases in terms of simple fabrication and use, low cost, high sensitivity and linear behaviour in a large domain of copper ion concentrations.

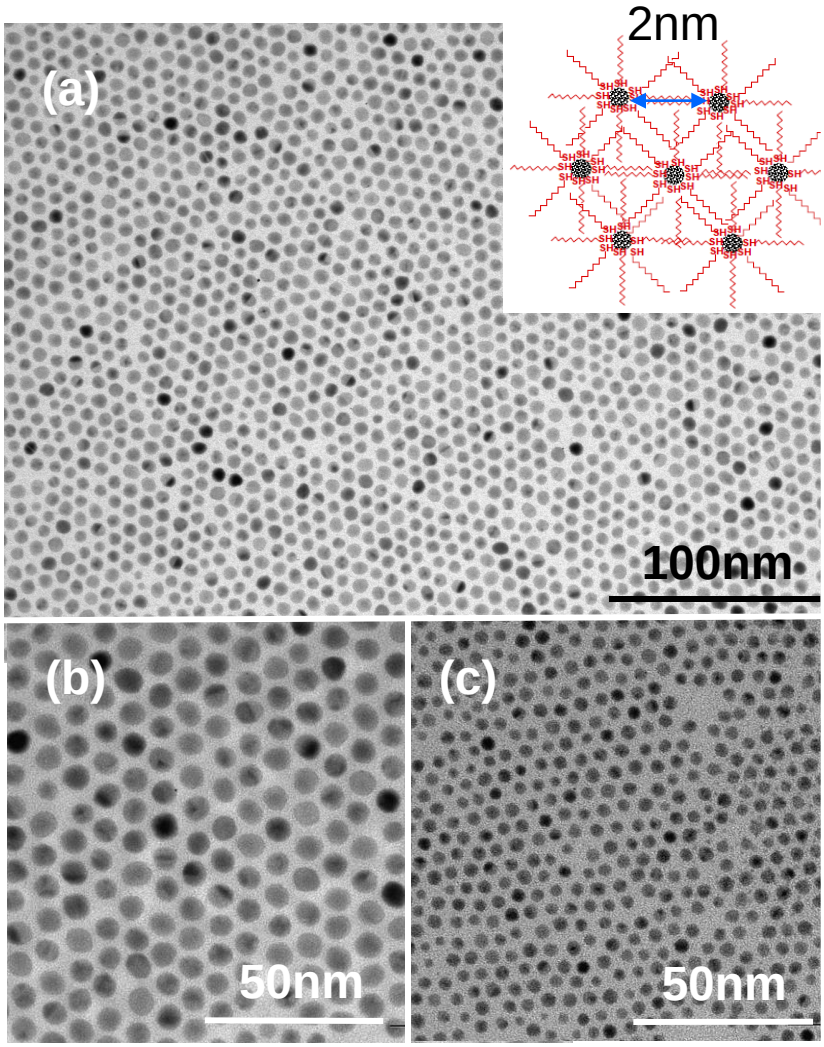

Figure 1

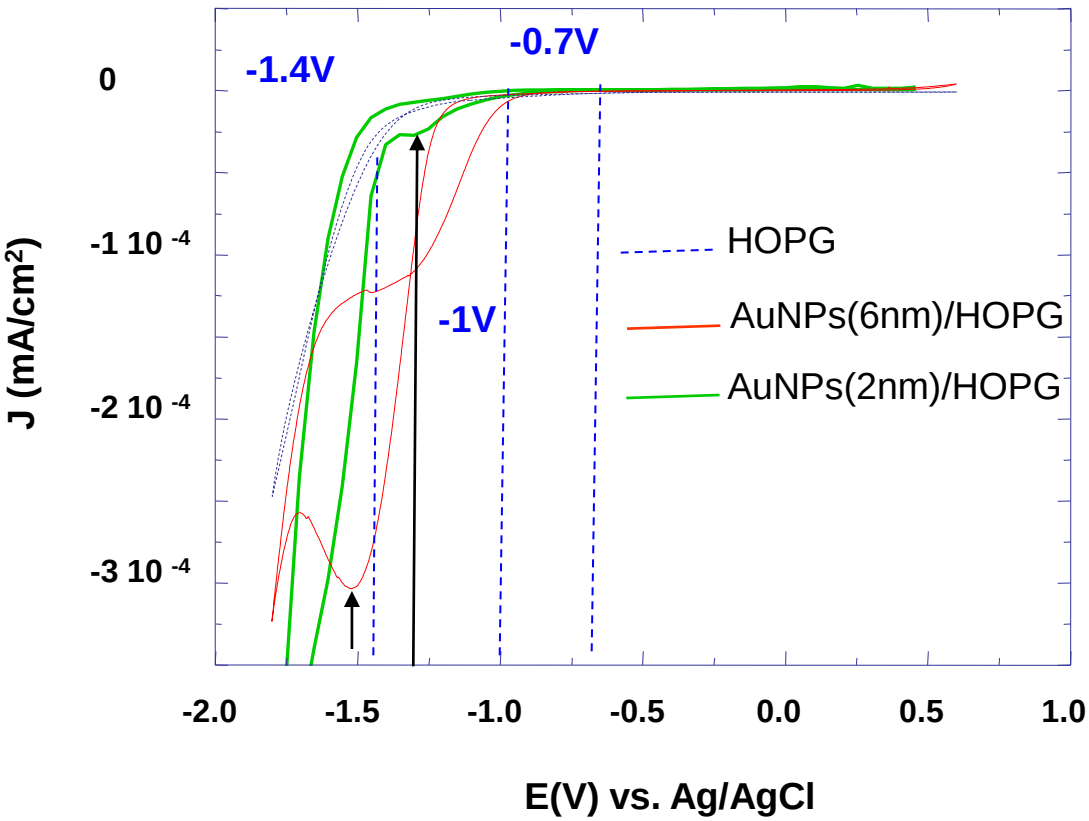
-1.4V
-0.7V
-1V
HOPG
AuNPs(6nm)/HOPG
AuNPs(2nm)/HOPG
J (mA/cm²)
0
-1 10 -4
-2 10 -4
-3 10 -4
-2.0
-1.5
-1.0
-0.5
0.0
0.5
1.0
E(V) vs. Ag/AgCl

Figure 2

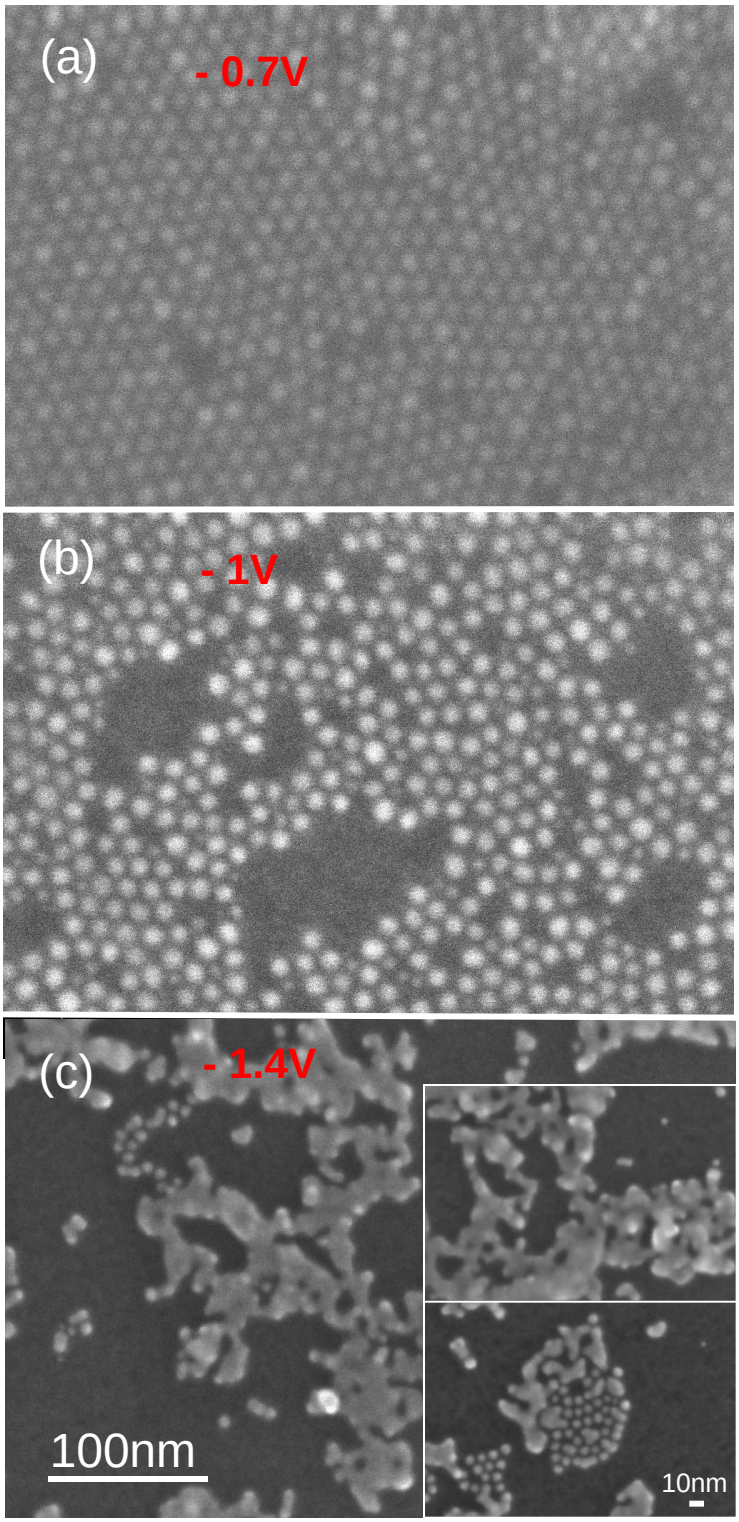

Figure 3

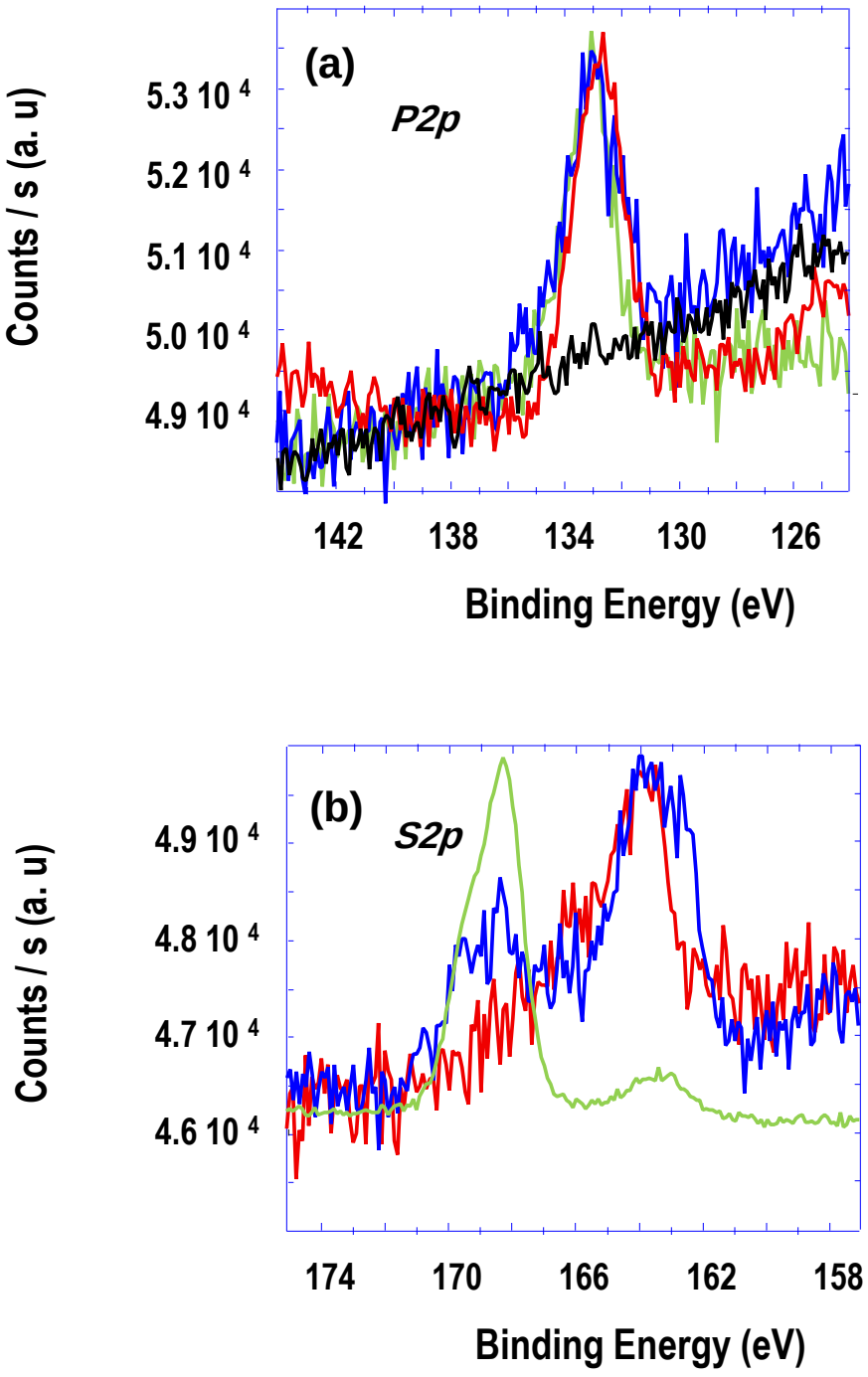
(a)
P2p
5.3 10 4
5.2 10 4
5.1 10 4
5.0 10 4
4.9 10 4
Counts / s (a. u)
142
138
134
130
126
Binding Energy (eV)
(b)
S2p
4.9 10 4
4.8 10 4
4.7 10 4
4.6 10 4
Counts / s (a. u)
174
170
166
162
158
Binding Energy (eV)

Figure 4

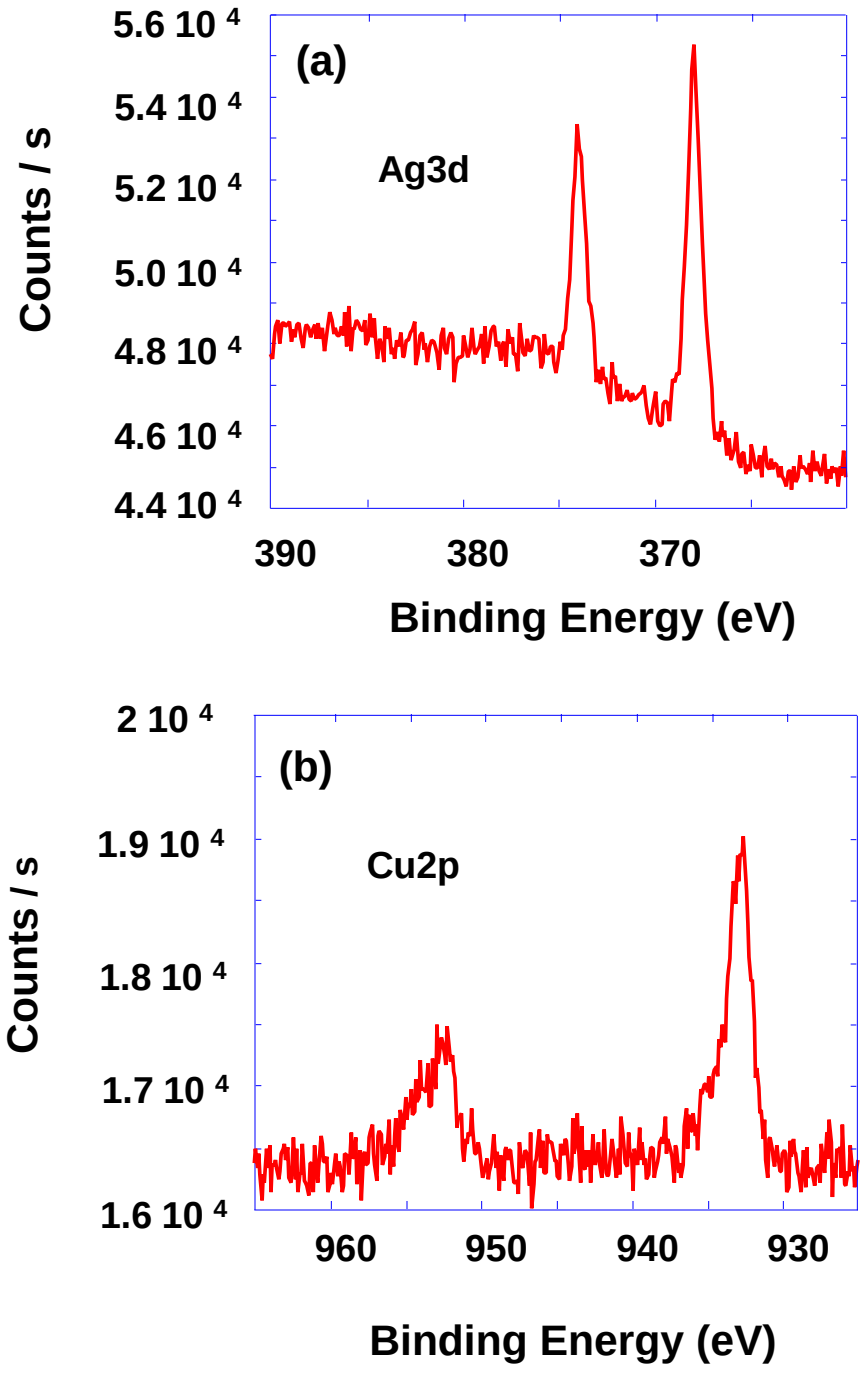
(a)
Ag3d
Counts / s
5.6 10 4
5.4 10 4
5.2 10 4
5.0 10 4
4.8 10 4
4.6 10 4
4.4 10 4
390
380
370
Binding Energy (eV)
(b)
Cu2p
Counts / s
2 10 4
1.9 10 4
1.8 10 4
1.7 10 4
1.6 10 4
960
950
940
930
Binding Energy (eV)

Figure 5

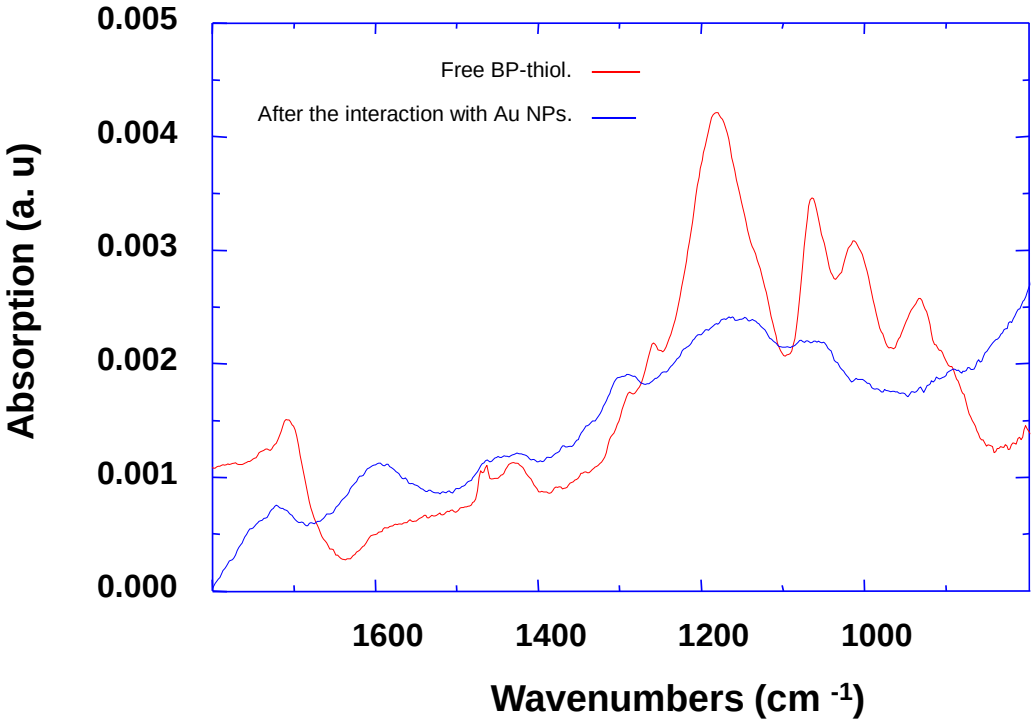
0.005
0.004
0.003
0.002
0.001
0.000
Absorption (a. u)
Free BP-thiol.
After the interaction with Au NPs.
1600
1400
1200
1000
Wavenumbers (cm -1)

Figure 6

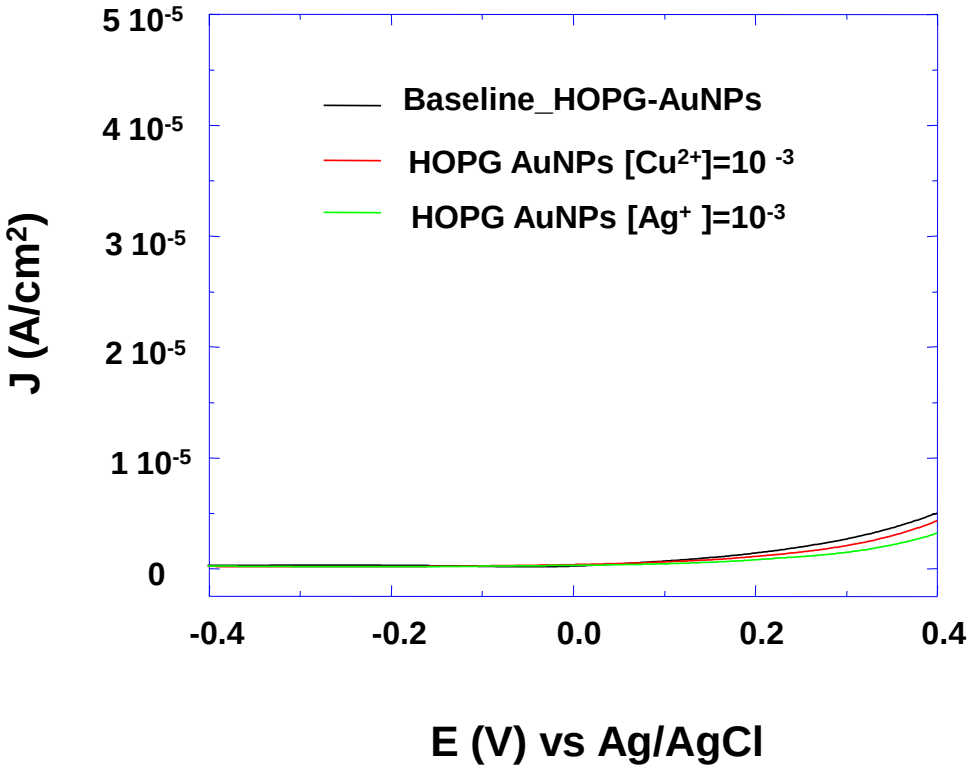
5 10-5
4 10-5
3 10-5
2 10-5
1 10-5
0
J (A/cm2)
Baseline_HOPG-AuNPs
HOPG AuNPs [Cu2+]=10 -3
HOPG AuNPs [Ag+]=10-3
-0.4
-0.2
0.0
0.2
0.4
E (V) vs Ag/AgCl

Figure 7

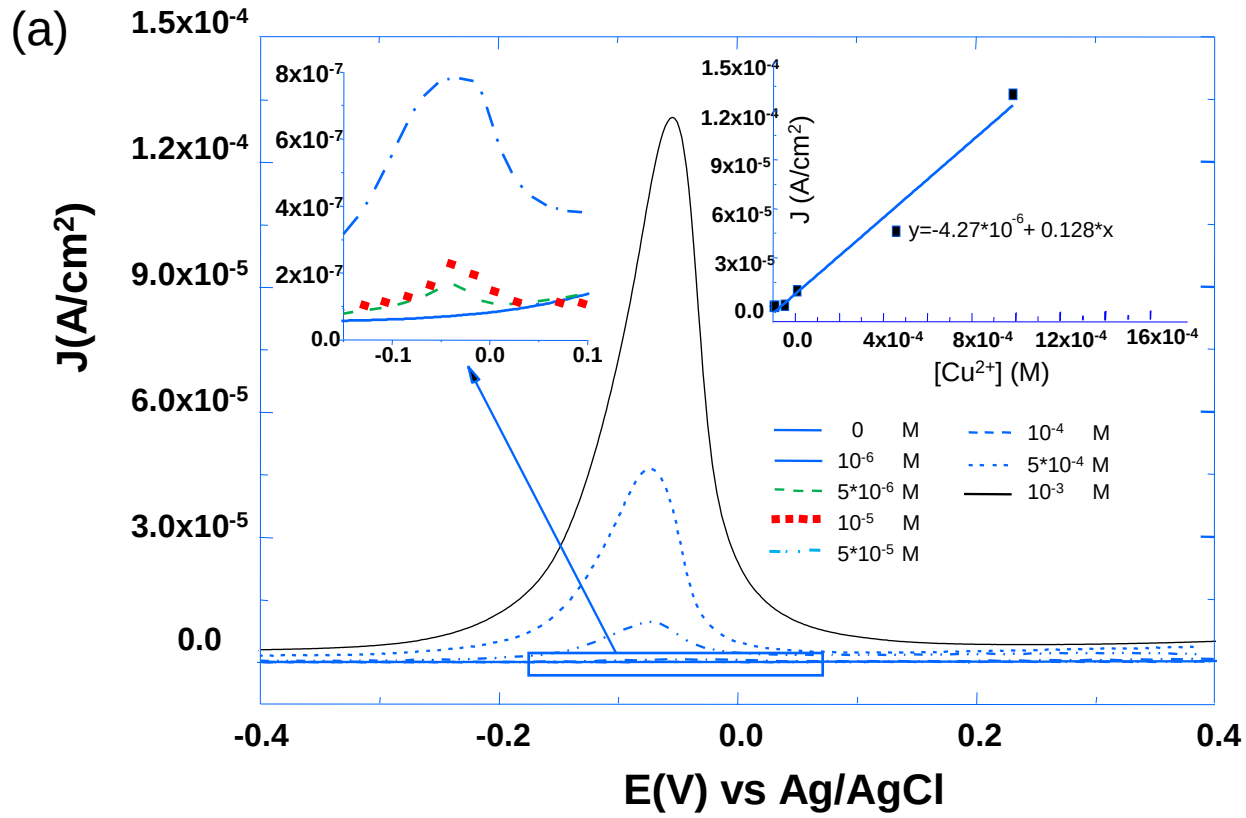
(a)
J(A/cm²)
E(V) vs Ag/AgCl
J (A/cm²)
y=-4.27*10⁻⁶+ 0.128*x
[Cu²⁺] (M)
0 M
10⁻⁶ M
5*10⁻⁶ M
10⁻⁵ M
5*10⁻⁵ M
10⁻⁴ M
5*10⁻⁴ M
10⁻³ M

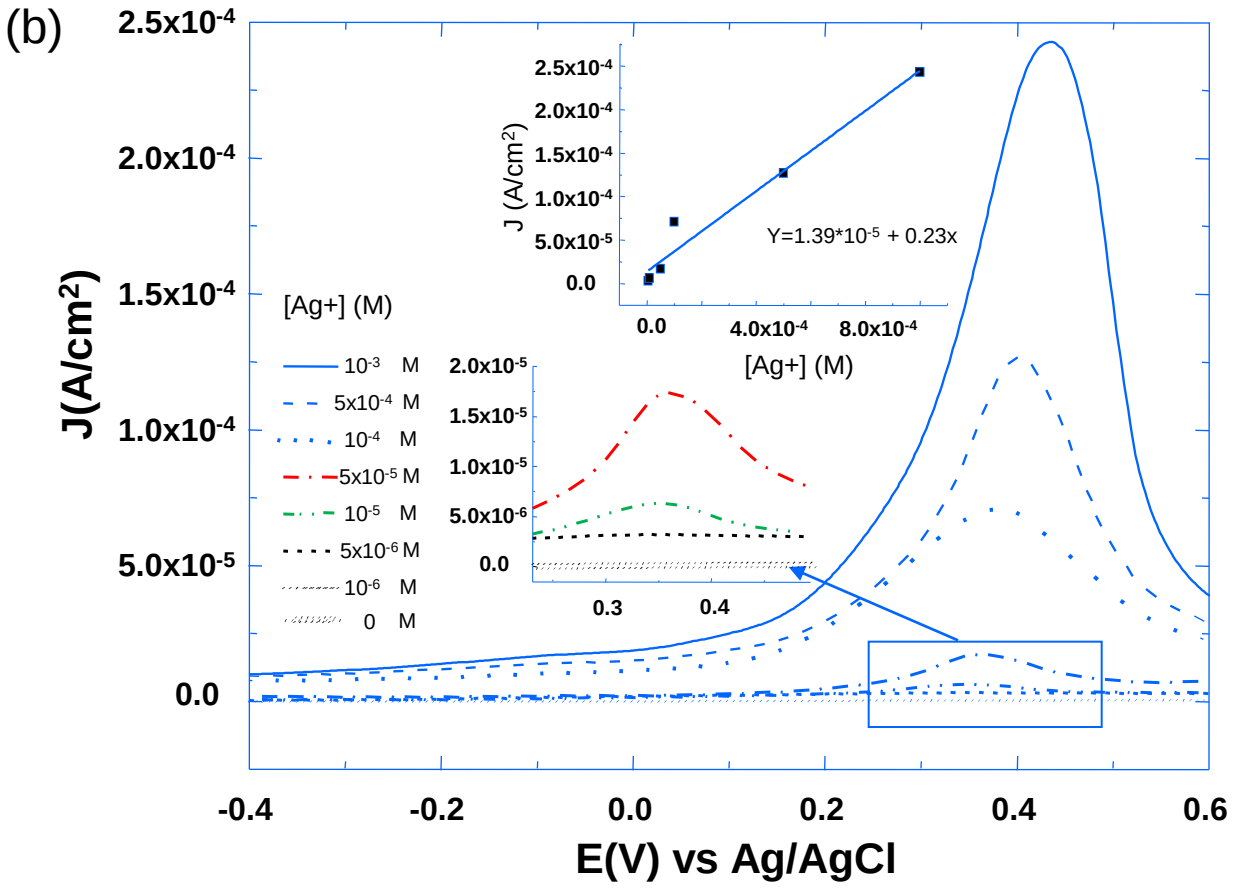
(b)
J(A/cm²)
E(V) vs Ag/AgCl
J (A/cm²)
Y=1.39*10⁻⁵ + 0.23x
[Ag+] (M)
[Ag+] (M)
10⁻³ M
5x10⁻⁴ M
10⁻⁴ M
5x10⁻⁵ M
10⁻⁵ M
5x10⁻⁶ M
10⁻⁶ M
0 M

Figure 8

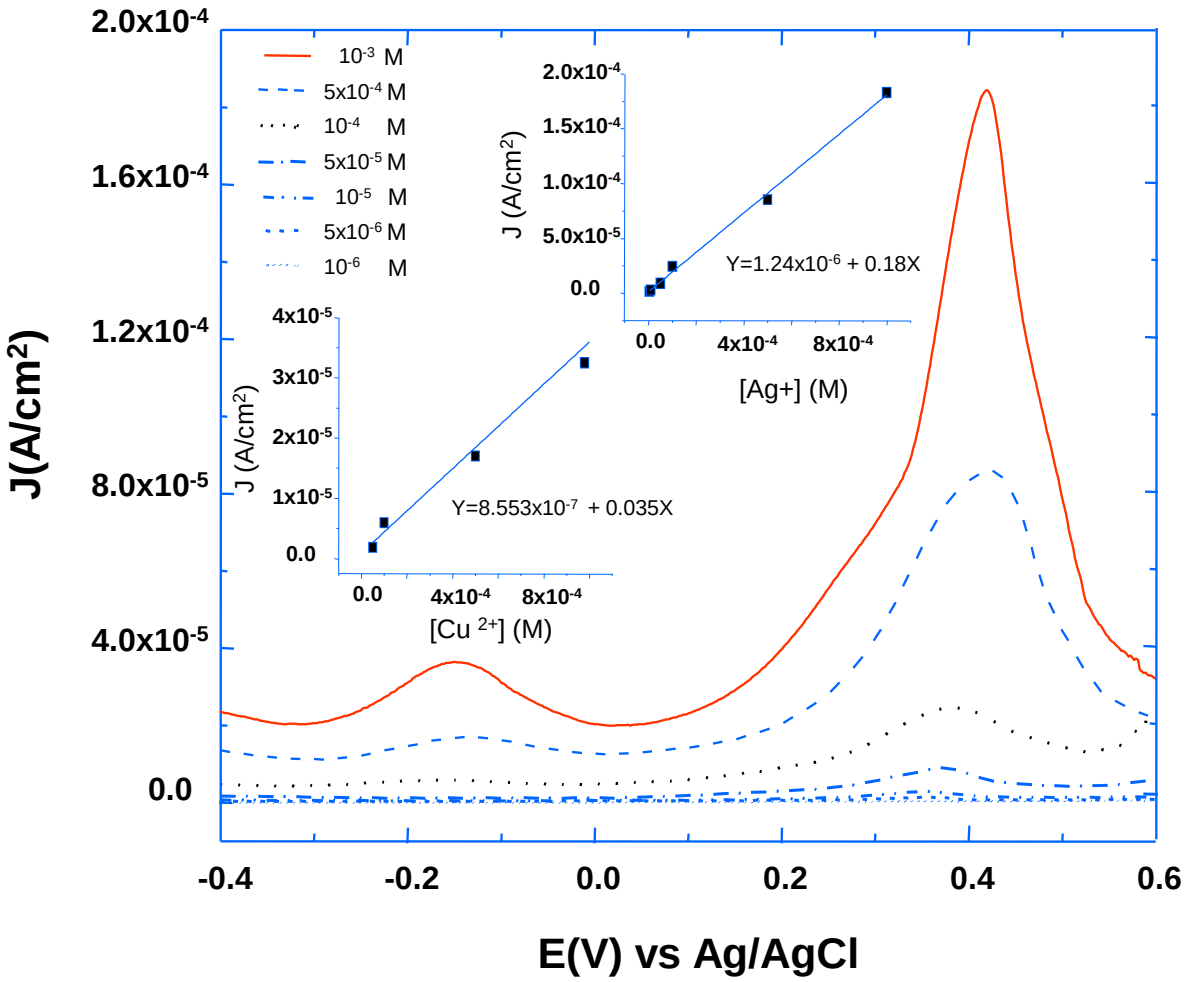
2.0x10-4
1.6x10-4
1.2x10-4
8.0x10-5
4.0x10-5
0.0
J(A/cm2)
-0.4
-0.2
0.0
0.2
0.4
0.6
E(V) vs Ag/AgCl
10-3 M
5x10-4 M
10-4 M
5x10-5 M
10-5 M
5x10-6 M
10-6 M
J (A/cm2)
Y=1.24x10-6 + 0.18X
[Ag+] (M)
Y=8.553x10-7 + 0.035X
[Cu 2+] (M)

Figure 9

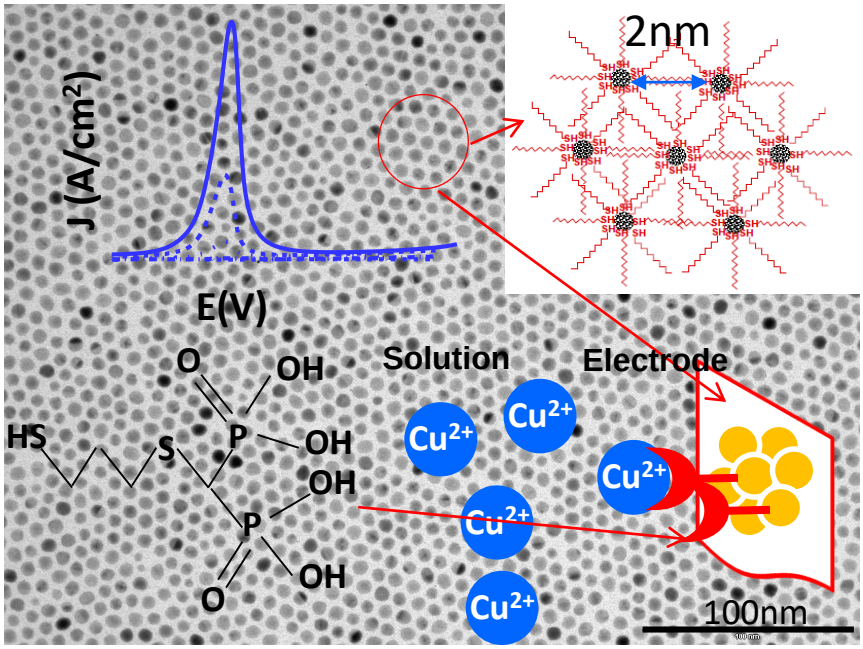

Self-organized gold nanoparticles modified HOPG was demonstrated to be a stable and a performing electrode material for electrochemical nanosensing devices.